Comparison of the Salt-Dependent Self-Association of Brain and Erythroid Spectrin†

Gillian E. Begg,‡ Michael B. Morris,§ and Greg B. Ralston*,‡

Departments of Biochemistry and Pharmacy, University of Sydney, Sydney NSW 2006, Australia

Received January 27, 1997; Revised Manuscript Received April 10, 1997⊗

ABSTRACT: The self-association of ovine brain spectrin in 0.1−1.5 M NaCl (pH 7.5) was studied using sedimentation velocity and sedimentation equilibrium techniques. Brain spectrin is tetrameric at sedimentation equilibrium at a 0.13 M ionic strength at 18−37 °C and at ionic strengths of up to 0.33 M at 20 °C. At ionic strengths greater than 0.33 M at 20 °C, the brain spectrin tetramer is destabilized, resulting in both dissociation to dimers and indefinite association to higher oligomers, in a manner similar to that seen with erythroid spectrin. The equilibrium constants describing all steps in the association involving the addition of dimers are around 15-fold higher for brain spectrin than for erythroid spectrin, at ionic strengths of ≥0.43 M. We propose that the stronger association of brain spectrin compared to that of erythroid spectrin is due to a relative inability of brain spectrin to form closed dimers. Sedimentation velocity analysis confirms that brain spectrin readily forms open dimers and that the association of open dimers is not kinetically trapped even at 2 °C. Our results suggest that the destabilization of spectrin tetramers in high-ionic strength conditions is due to increased independent movement of the α and β subunits resulting from disruption of electrostatic interactions. The greater stability of brain spectrin oligomers relative to those of erythroid spectrin is due to stronger nonelectrostatic interactions which stabilize the rigidity of the individual subunits and thereby increase the conformational strain associated with dimer closure.

Brain spectrin is a member of a large family of membrane-associated, actin-cross-linking proteins. At least one spectrin isoform is found in the cytoskeletal structures of most vertebrate cells (*1*). Spectrins are highly elongated proteins, comprised of an α and a β subunit which associate laterally in an antiparallel manner to form a heterodimer and "head-to-head" to form a tetramer. Both subunits consist largely of a series of homologous repeating motifs, each approximately 106 residues in length (*2*). The structure of a repeat motif has been determined by X-ray crystallography (*3*) and NMR spectroscopy (*4*) to consist of a triple α-helical bundle. The lateral association of the subunits is initiated near the actin-binding end of the dimer, where two repeat motifs from each monomer bind strongly (*5*, *6*), and is followed by association of the subunits along their length, perhaps in a zipper-like manner (*5*). The head-to-head association of the subunits is achieved by the binding of complementary partial repeat motifs at the head of the α and β subunits which forms a complete repeat motif (*7*, *8*).

The self-association of spectrin dimers to tetramers is crucial to their role as proteins that cross-link actin and membrane domains; the spectrin dimer is monovalent for actin and therefore incapable of cross-linking actin filaments. The kinetics, thermodynamics, and mode of association of erythroid spectrin dimers have been well characterized (*9*−*11*). However, the characteristics of erythroid spectrin cannot necessarily be extrapolated to nonerythroid spectrins. Erythroid spectrin is capable of associating to oligomers higher than the tetramer in physiological conditions, through the sequential addition of heterodimers (*12*−*15*). In contrast, early studies of brain spectrin using sedimentation through sucrose gradients, electron microscopy, and nondenaturing PAGE[1] determined that this isoform existed only as a tetramer in <300 mM salt (*16*−*20*).

It has been thought that the differences in self-association behavior of erythroid and nonerythroid spectrin may be linked to their differing morphology (*21*). Electron micrographs of brain spectrin have shown that it is a straighter molecule than erythroid spectrin, with fewer gaps visible between the α and β subunits (*16*, *17*, *20*). The molecular basis for this is unknown; though the structure of the repeat motif has been solved, little is known of the structure and interactions between consecutive repeat motifs, or of the lateral interactions between the α and β chains, and the influence of these interactions on the morphology and self-association of spectrins.

In the present study, analytical ultracentrifugation has been used to examine the self-association of brain spectrin as a function of ionic strength. We have found that as the ionic strength is increased above 330 mM the brain spectrin tetramer is destabilized, leading to dissociation to dimers and indefinite association to higher oligomers via a mechanism similar to that for erythroid spectrin. At all ionic strengths used, the brain isoform shows a significantly reduced ability

† This study was supported by Australian National Health and Medical Research Council Dora Lush Scholarship 947413 to G.E.B. and an Australian Research Council grant to G.B.R.

* Correspondence should be addressed to this author at the Department of Biochemistry, University of Sydney, Sydney NSW 2006, Australia. Telephone: 61 2 9351 3906. Fax: 61 2 9351 4726. E-mail: G. Ralston@biochem.usyd.edu.au.

‡ Department of Biochemistry, University of Sydney.

§ Department of Pharmacy, University of Sydney.

⊗ Abstract published in *Advance ACS Abstracts,* May 15, 1997.

[1] Abbreviations: DTT, dithiothreitol; SDS−PAGE, sodium dodecyl sulfate−polyacrylamide gel electrophoresis; FPLC, fast process liquid chromatography; CD, circular dichroism.

S0006-2960(97)00186-4 CCC: $14.00

to form closed dimers and a greater strength of association relative to erythroid spectrin. The implications of the data for the interactions stabilizing both isoforms of spectrin are discussed.

EXPERIMENTAL PROCEDURES

Purification of Brain Spectrin. Brain spectrin was prepared from approximately 150 g of ovine brain using the method of Bennett *et al.* (*22*), with the following modifications. Protein was precipitated from the low-ionic strength extract by addition of 0.35 g/mL ammonium sulfate at 2 °C. The suspension was kept at 4 °C overnight and then at −10 °C for 1 h before centrifugation for 15 min at 25000*g*. The precipitate was resuspended in 12 mL of gel filtration buffer (1 M NaBr, 10 mM sodium phosphate, 1 mM Na_2EGTA, 15 mM sodium pyrophosphate, 0.02% NaN_3, and 0.4 mM DTT at pH 8.2) and dialyzed against 400 mL of the same buffer for 4 h at 4 °C. The suspension was centrifuged for 60 min at 180000*g*, the supernatant applied to a Sepharose CL-4B column (2.5 × 90 cm) equilibrated with gel filtration buffer, and the protein eluted using a flow rate of 20 mL/h. Fractions were monitored using the absorbance at 280 nm and were examined by means of SDS−PAGE. Spectrin fractions were pooled and dialyzed against 2.5 L of buffer A (50 mM NaCl, 10 mM sodium phosphate, 0.5 mM Na_2EDTA, and 0.5 mM DTT at pH 6.8) for 3 h. The pooled fractions were concentrated against Aquacide II (Calbiochem) to 5−8 mL and dialyzed overnight against 2.5 L of buffer A. FPLC was used to further purify the brain spectrin. The dialyzed protein was centrifuged for 25 min at 35000*g*, and the supernatant injected onto a Mono Q HA 5/5 anion exchange column (Pharmacia) equilibrated with buffer A. Spectrin was eluted at 0.5 mL/min with a 30 mL linear gradient of buffer A versus buffer B (1 M NaCl, 10 mM sodium phosphate, 0.5 mM EGTA, and 0.5 mM DTT at pH 6.8). The 0.5 mL fractions were monitored using the absorbance at 280 nm and were examined by means of SDS−PAGE.

Human erythroid spectrin was purified as described by Morris and Ralston (*10*).

Preparation of Spectrin Samples for Ultracentrifugation. For both brain and erythroid spectrin, fractions from the middle of the chromatography peaks were pooled and, where necessary, concentrated using centrifugal concentrators. Samples were then dialyzed for 4−16 h at 4 °C in a buffer comprised of 10 mM sodium phosphate and 1 mM EGTA at pH 7.5 which included 0.1−2.0 M NaCl. Prior to dialysis, all buffers were purged with nitrogen to remove dissolved oxygen, and DTT (0.2−1.0 mM) was added. For samples analyzed by sedimentation equilibrium at temperatures above 30 °C, 1% w/v metrizamide (Sigma Chemical Co.) was included in the buffer to stabilize the protein concentration gradient (*23*).

Sedimentation Velocity. Sedimentation velocity experiments were performed using a Beckman XL-A analytical ultracentrifuge fitted with absorbance optics. Samples (~0.2 mg/mL spectrin) were loaded into cells fitted with double-sector 12 mm centerpieces, equilibrated to the temperature of the experiment for up to 1 h, and centrifuged at 40 000 rpm. The program VELGAMMA (Beckman) was used to calculate the rate of movement of the second moment of the boundary and the rate of spreading of the boundary, in order to determine the weight-average sedimentation coefficient, s, and diffusion coefficient, D, respectively. These coefficients were then corrected for the effects of ionic strength and temperature on the viscosity and density of the solution to give the equivalent values in water, $s_{20,w}$ and $D_{20,w}$.

Sedimentation Equilibrium. Meniscus depletion sedimentation equilibrium experiments were performed on a Beckman-Spinco model E analytical ultracentrifuge at 18−37 °C. The ultracentrifuge cells were fitted with Yphantis-style, six-channel centerpieces and loaded with three different concentrations of spectrin (typically 0.2, 0.4, and 0.8 mg/mL). The samples were centrifuged at 6000−10000 rpm for up to 90 h. Photographs of the Rayleigh interference pattern were taken at zero time and at intervals after 24 h and were measured using a Nikon comparator linked to an automated plate reader. Measurements were baseline corrected by subtracting the zero-time data (*24*). Concentration (c) versus radius (r) data were calculated using a conversion factor of 4.04 fringes for every 1 g/L protein (*25*).

Sedimentation Equilibrium Data Treatment and Model Fitting.[2] The experimental data were treated in two ways. From ln $c(r)$ versus r^2 data, apparent point-average weight-average molecular weight values ($M_{w,app}$) were calculated (*24*). In addition, the concentration versus radius data were transformed using the Ω function, $\Omega(r)$ (*26*):

$$\Omega(r) = \frac{c(r)\exp[\phi_1 M_1(r_F^2 - r^2)]}{c(r_F)} \quad (1a)$$

$$= \frac{a_1(r_F)c(r)}{a_1(r)c(r_F)} \quad (1b)$$

where $\phi = (1 - \bar{\nu}\rho)\omega^2/2RT$, where $\bar{\nu}$ is the partial specific volume of the protomer in milliliters per gram, ρ the density of the solvent in grams per milliliter and ω the angular velocity in radians per second. M_1 is the molar mass of the protomer; $c(r)$ and $c(r_F)$ are the total protein concentrations (grams per liter) at radial position r and the reference position r_F, respectively, and a_1 is the thermodynamic activity of the protomer. In calculation of $\Omega(r)$, a value of 0.73 mL/g was used for $\bar{\nu}$ at 20 °C [calculated from the cDNA sequence of Ma *et al.* (*27*) and Wasenius *et al.* (*28*)]. Values of $\bar{\nu}$ at other temperatures were calculated according to Laue *et al.* (*29*). The value of ρ was also calculated for each solvent and temperature (*29*). The molecular weight of the protomer, M_1, was taken to be 559 000 (calculated from cDNA sequence data) where the protomer of the reaction was the heterodimer. In experiments where a significant proportion of monomer was detected, a protomer molecular weight of 280 000 was used, i.e., the average molecular weight of the α and β chains.

Plots of $\Omega(r)$ versus $c(r)$ for the three loading concentrations of protein at sedimentation equilibrium were calculated using a common value of $c(r_F)$. Overlap of the data over the common concentration range is a very sensitive indicator that both chemical and sedimentation equilibrium have been attained (*26*, *30*). The Ω data were fitted with models of indefinite association—SEK 1, SEK 3, and SEK 4 (*31*)—pre-

[2] A package of programs for the workup of raw data and for the fitting of models is available via anonymous FTP at the address bbri.harvard.edu. Change to directory rasmb.spin.ms_dos.sedprog-ralston.

viously used to describe erythroid spectrin self-association (e.g., *32*, *33*). For each model, the concentration of the protomer, $c_1(r)$, can be written as an implicit function of $c(r)$.

The SEK 1 model describes the sequential addition of protomers (in this case, dimers), where the addition of each dimer is described by a single molar equilibrium constant, K:

$$D \overset{K}{\rightleftharpoons} D_2 \overset{K}{\rightleftharpoons} D_3 \overset{K}{\rightleftharpoons} D_4 \overset{K}{\rightleftharpoons} ... \rightleftharpoons D_n$$

$$c(r) = c_1(r)/[1 - kc_1(r)]^2 \quad \text{if } kc_1(r) < 1 \quad \text{where } k = K/M_1 \quad (2)$$

In the SEK 3 model, the dimer−tetramer equilibrium constant is described separately by K_{24}, and every subsequent addition of dimer is described by K_{iso}.

$$D \overset{K_{24}}{\rightleftharpoons} D_2 \overset{K_{iso}}{\rightleftharpoons} D_3 \overset{K_{iso}}{\rightleftharpoons} D_4 \rightleftharpoons ... \rightleftharpoons D_n$$

$$c(r) = c_1(r)\left\{1 + \frac{k_{24}c_1(r)[2 - k_{iso}c_1(r)]}{[1 - k_{iso}c_1(r)]^2}\right\} \quad \text{if } k_{iso}c_1(r) < 1$$

$$\text{where } k_{iso} = K_{iso}/M_1 \text{ and } k_{24} = K_{24}/M_1 \quad (3)$$

In the SEK 4 model, all additions of dimer are described by a single K (as for SEK 1). However, the association of monomers to form the dimer is also included and is described by K_{12}:

$$2M \overset{K_{12}}{\rightleftharpoons} D \overset{K}{\rightleftharpoons} D_2 \overset{K}{\rightleftharpoons} D_3 \overset{K}{\rightleftharpoons} ... \rightleftharpoons D_n$$

$$c(r) = c_1(r)\left\{1 + \frac{2k_{12}c_1(r)}{[1 - k_{12}kc_1(r)^2]^2}\right\}$$

$$\text{where } k_{12} = K_{12}/M_1 \text{ and } k = K/M_1 \quad (4)$$

For all models, the Adams−Fujita approximation (*34*) was used to relate the thermodynamic activity of the protomer, $a_1(r)$, to the concentration of the protomer $c_1(r)$:

$$a_1(r) = c_1(r) \exp[BM_1c(r)] \quad (5)$$

where B, the second virial coefficient, is a measure of the nonideality of the solute.

The models were fitted to the Ω function curves by nonlinear regression as described (*30*, *32*). The regression program returned the approximate (asymptotic) standard errors of the variable parameters calculated from the inverse matrix set up from partial derivative equations of the fitting function (*35*).

In cases where the Ω data showed no evidence of association, the program NONLIN (*36*) was used to fit the *c(r)* versus *r* data with a single nonideal species model, which gave an estimate of the molecular weight of the species, and its nonideality, B.

Circular Dichroism. CD spectra were measured at 25 °C over the wavelength range of 200−260 nm using a Jasco J-720 spectropolarimeter and 1 mm path length cells. Samples of erythroid or brain spectrin (∼1.5 mg/mL) were dialyzed in 10 mM sodium phosphate, 0.1 M NaCl, 0.5 mM EGTA, and 0.5 mM DTT at pH 7.5 and then diluted to 0.1 mg/mL protein with buffers containing 10 mM sodium phosphate and 0.1−2.0 M NaCl at pH 7.5 at least 1 h prior to measurement. The data obtained were converted to mean residue ellipticity (*37*) using a mean residue weight of 115.2 for erythroid spectrin and 115.5 for brain spectrin.

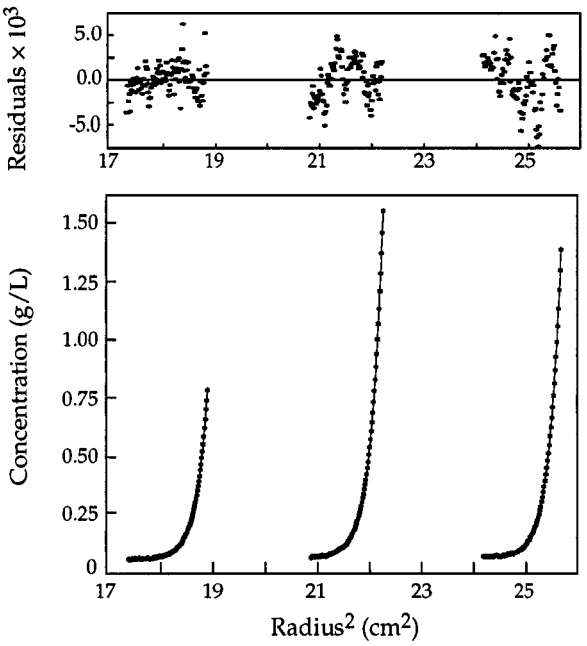

FIGURE 1: (Lower panel) Concentration versus radius data for three loading concentrations of brain spectrin at sedimentation equilibrium in 10 mM phosphate, (pH 7.5) and 0.1 M NaCl at 32 °C. The three data sets were fitted simultaneously by a single-nonideal species model using the nonlinear regression program NONLIN (*36*). The calculated fit is represented by the solid line. For this set of data, the returned value of the protomer molecular weight $M_1 = (1.16 \pm 0.03) \times 10^6$ and that of the nonideality parameter $B = (8.8 \pm 1.7) \times 10^{-8}$ L mol g^{-2}. (Upper panel) Plot of the residuals of the fitted curve to the data points for each data set.

RESULTS

Sedimentation Equilibrium Analysis of Brain Spectrin Tetramer. The $c(r)$ versus r data of brain spectrin in 100 mM NaCl at 18−37 °C, and 200−300 mM NaCl at 18−30 °C, were analyzed directly using the nonlinear regression program NONLIN (*36*). In all cases, the data were best fit by a model describing a single nonideal species (Figure 1). The returned value of the molecular mass, averaged over nine experiments, was $(1.14 \pm 0.03) \times 10^6$ Da and is consistent with the molecular mass of the brain spectrin tetramer calculated from the cDNA sequence of 1.12×10^6 Da (*27*, *28*).

The second virial coefficient, B, a measure of the nonideality of the molecule, was also estimated by the fitting program for each experiment, and the average value obtained was $(0.80 \pm 0.22) \times 10^{-7}$ L mol g^{-2}. A theoretical B may be calculated (*38*) by combining the nonideality arising from the charge of the molecule (at the experimental pH) with the nonideality arising from the excluded volume of the molecule, which is dependent upon the molecule's size and shape. Theoretical B values were calculated for brain spectrin modeled as a stiff rod (200 nm long, 3 nm diameter) and as an expanded sphere with a Stokes radius of 22.0 nm (calculated from the sedimentation coefficient) using the equations of Tanford (*38*). The estimated maximum charge on the tetramer at pH 7.5 is −339, calculated using standard residue pK_a values. However, this can be reduced markedly

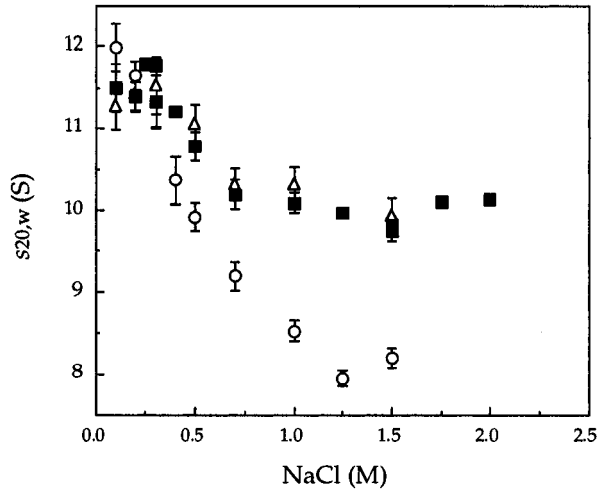

FIGURE 2: Ionic strength dependence of the weight-average sedimentation coefficient, $s_{20,w,}$ of brain spectrin at 2 (△), 20 (■), and 37 °C (○). Values of the sedimentation coefficient were determined from the rate of movement of the second moment of the boundary using the program VELGAMMA and corrected for the effect of salt and temperature on the density and viscosity of the solution to give $s_{20,w}$. The error bars represent the standard error of the measurement.

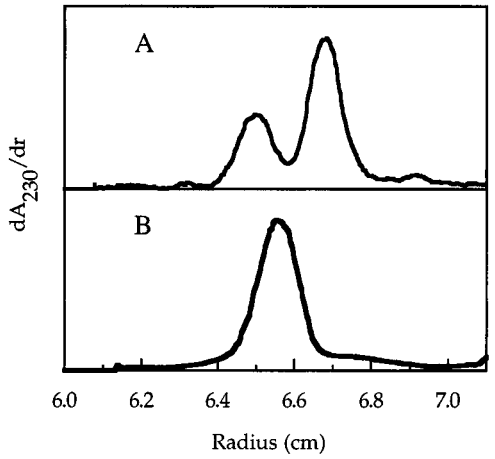

FIGURE 3: Comparison of boundaries formed during sedimentation velocity experiments of erythroid and brain spectrin at 20 °C in 0.5 M NaCl and 10 mM phosphate at pH 7.5. The boundaries were recorded using absorbance optics at 230 nm, and the absorbance was differentiated with respect to the radial distance to provide plots reflecting the concentration gradient versus radial distance. (A) Erythroid spectrin forms separate dimer and tetramer boundaries due to slow interconversion of the species. (B) Brain spectrin forms a single boundary with a weight-average sedimentation coefficient lying between that of the dimer and tetramer, indicating rapid interconversion of these species on the time scale of the experiment.

by counterion binding. Therefore, a value of 50 ± 20% of the maximum charge was used (*38*). The calculated value of *B* for the rod was 1.91 (1.25, 2.90) × 10^{-7} L mol g^{-2}, while that for the sphere was 2.68 (2.04, 3.68) × 10^{-7} L mol g^{-2}. These theoretical values are closely similar to the experimental values of *B*. The small differences may occur because the model shapes are not entirely appropriate, the level of counterion binding exceeds 70%, or there is a very small percentage of high-molecular weight oligomers present, which would artificially reduce the experimentally derived value of *B*.

Sedimentation Velocity of the Brain Spectrin Tetramer. Sedimentation velocity experiments were also performed on the brain spectrin tetramer in 0.1 M NaCl at 20 °C. Values for $s_{20,w}$ of 11.7 S and frictional ratio f/f_o of 3.3 were obtained. When compared with values obtained for the erythroid spectrin tetramer ($s_{20,w}$ = 13.7 S, f/f_o = 2.7), the results indicate that brain spectrin is a more asymmetric molecule than erythroid spectrin. These results are qualitatively (but not quantitatively) similar to those obtained using sucrose gradients (*17*, *18*) and are consistent with the straighter, more rigid appearance of brain spectrin in electron micrographs (*16*, *17*, *20*).

Destabilization of the Brain Spectrin Tetramer at High Ionic Strengths. To investigate the stability of brain spectrin as a function of ionic strength and temperature, sedimentation velocity experiments were performed at 2, 20, and 37 °C in 0.1−2.0 M NaCl and 10 mM sodium phosphate at pH 7.5 (Figure 2). Brain spectrin in 0.1 M NaCl sedimented as a single boundary at all temperatures examined, as expected for a single (tetrameric) species.

As the concentration of NaCl increased, brain spectrin continued to sediment as a single boundary (e.g., see Figure 3B). However, the weight-average sedimentation coefficient decreased, undergoing a transition between 0.3 and 1.5 M NaCl (Figure 2). The transition is not due to a salt-dependent shape change in the tetramer, since the ratio of $s_{20,w}$ to the diffusion coefficient, $D_{20,w}$, decreased, indicating a decrease in the average molecular weight. The decrease in $s_{20,w}$ therefore reflects dissociation of the brain spectrin tetramer to one or more smaller species with increasing ionic strengths.

The composition of the samples cannot be precisely quantified from the ratio of $s_{20,w}$ and $D_{20,w}$, due to artificial broadening of the boundary arising from the presence of more than one species. However, the transitions at 2 and 20 °C do not reach $s_{20,w}$ values lower than that of the erythroid spectrin dimer (9.9 S), indicating that increasing the concentration of salt promotes a dimer−tetramer exchange. The transition at 37 °C indicates dissociation far greater than that at the lower temperatures, with the $s_{20,w}$ values falling to ∼8 S. Using the ratio of $s_{20,w}$ values of the erythroid and brain spectrin tetramer as a guide, the sedimentation coefficient of the brain spectrin dimer is predicted to be ∼8.5 S. Thus, at 37 °C, the data indicate complete dissociation of brain spectrin tetramers to dimers, and possibly some dissociation to monomers in ≥1.0 M NaCl.

Kinetics of Brain Spectrin Dimer−Tetramer Exchange. The presence of a single sedimenting boundary throughout the salt-dependent transition demonstrates that the brain spectrin dimers and tetramers undergo rapid exchange even at 2 °C. This is in marked contrast to erythroid spectrin, for which the kinetics of self-association are very slow at 21 °C, and immeasurably slow below 10 °C (*9*), resulting in the formation of separate boundaries for the dimer and tetramer during sedimentation velocity experiments performed at ≤25 °C in 0.1 M salt. In fact, we have found that erythroid spectrin forms separate tetramer and dimer boundaries at 20 °C in ≤0.5 M NaCl, and the sedimentation coefficients are not significantly reduced relative to those obtained in 0.1 M NaCl (Figure 3A).

The slow interconversion of erythroid spectrin dimers and tetramers in the cold is due to a very high activation barrier which is thought to arise from conformational strain associated with the formation of the "closed" dimer from an "open"

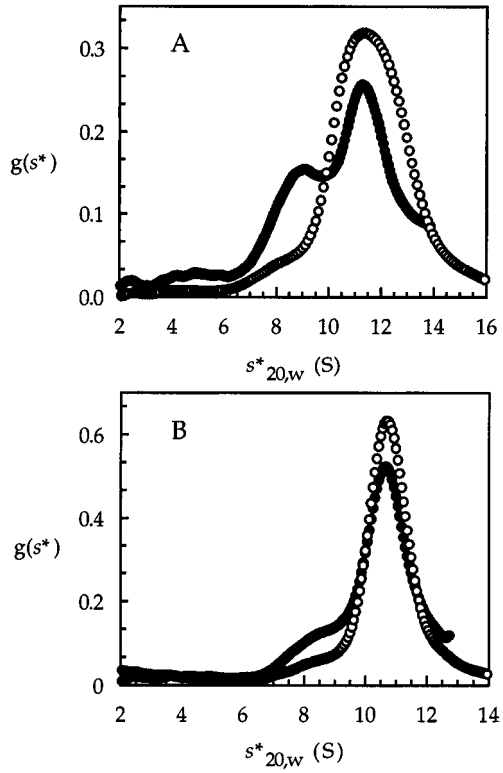

FIGURE 4: Sedimentation velocity results reflecting the formation of closed dimers of brain spectrin. The plots show the distribution of the apparent sedimentation coefficient, $g(s^*)$, normalized to the area under the boundary. (A) Brain spectrin incubated at 20 (○) and 37 °C (●) in 10 mM sodium phosphate buffer and 0.5 M NaCl at pH 7.5 for 20 h prior to sedimentation velocity analysis at 20 °C. Following the heating of brain spectrin to 37 °C, a separate boundary is formed with a value of $s_{20,w}$ (8.7 S) consistent with that predicted for the brain spectrin dimer. (B) Brain spectrin incubated at 20 °C for 0 (○) and 80 h (●) in 10 mM sodium phosphate buffer and 1.0 M NaCl at pH 7.5 prior to sedimentation velocity analysis at 20 °C. By 80 h of incubation, a shoulder appears which can be resolved as a second boundary ($s_{20,w}$ = 8.1 S) after extrapolation of the $g(s^*)$ distribution to infinite time.

dimer (*7*, *10*, *39*). A dimer is closed when the self-association binding sites of the α and β subunits are associated within the dimer. This intradimer bond must be broken before tetramers can form. The rapid exchange of brain spectrin dimers and tetramers therefore suggests that the single boundary represents the interconversion of *open* dimers with tetramers, or alternatively, that brain spectrin closed dimers are not kinetically trapped.

To determine if brain spectrin is able to form closed dimers, a sample of brain spectrin in 0.5 M NaCl was incubated at 37 °C for 20 h (to increase the proportion of dimers and to overcome any activation barrier to dimer closure), then chilled on ice, and sedimented at 20 °C. The distribution of the apparent sedimentation coefficient, $g(s^*)$, was calculated (*40, 41*) to improve the resolution of boundaries formed in the sample. In contrast to the control sample incubated at 20 °C, the sample incubated at 37 °C clearly formed two boundaries (Figure 4A) with sedimentation coefficients of ∼11.4 S (corresponding to a reaction boundary representing tetramer−open dimer exchange) and ∼8.7 S (close to the predicted coefficient of the dimer). This demonstrated that at higher temperatures brain spectrin can form closed dimers which can be kinetically trapped at 20 °C.

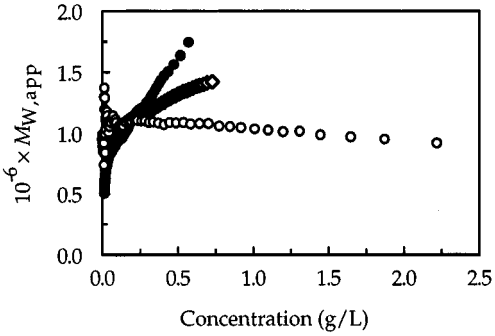

FIGURE 5: Apparent weight-average molecular weight, $M_{W,app}$, versus protein concentration data obtained from sedimentation equilibrium experiments of brain spectrin at 20 °C in 10 mM sodium phosphate at pH 7.5 and 0.1 (○), 0.5 (◇), or 1.5 M (●) NaCl. Three different loading concentrations of protein at each ionic strength were sedimented to simultaneous chemical and sedimentation equilibrium as verified by the overlap of plots of $M_{W,app}$ versus concentration and Ω versus concentration. Data from the three loading concentrations for each ionic strength were then averaged three points at a time.

The propensity of brain spectrin to form closed dimers at 20 °C was then investigated by sedimenting samples which had been dialyzed against 1.0 M NaCl at 4 °C and then incubated at 20 °C for up to 80 h. As Figure 4B shows, a single boundary representing the tetramer−open dimer exchange is seen after 0 h at 20 °C. However by 80 h of incubation, a shoulder has developed on the trailing edge of the main boundary. After extrapolation of the $g(s^*)$ distribution to infinite time (*40*), the second boundary was resolved, with an $s_{20,w}$ of ∼8.1 S, demonstrating that a small proportion of closed dimers are formed.

Sedimentation Equilibrium Analysis of Brain Spectrin Self-Association at High Ionic Strengths. The dependence of the association behavior of brain spectrin on ionic strength at 20 °C was quantified by sedimentation equilibrium analysis. The apparent weight-average molecular weight ($M_{w,app}$) versus concentration data in Figure 5 show that, as the NaCl concentration increases above 0.3 M, the value of $M_{w,app}$ at zero protein concentration becomes smaller than that of the tetramer, confirming the dissociation of brain spectrin tetramers to dimers. However, at protein concentrations higher than 0.3 g/L, the value of $M_{w,app}$ increases well above that of the tetramer, indicating self-association to larger oligomers.

To determine the pattern of self-association, Ω distributions were generated from $c(r)$ versus r data obtained for brain spectrin in 0.4−1.5 M NaCl. Good overlap of the Ω curves for the three loading concentrations of protein in each experiment indicated that chemical and sedimentation equilibrium had been reached and that all species present participated in the equilibrium. Initial attempts to fit the data used the discrete models DTH (dimer−tetramer−hexamer) and DTHO (dimer−tetramer−hexamer−octamer), where each equilibrium constant is defined independently. The fit of the DTH model to the 0.4−1.5 M NaCl data was consistently poor, with a nonrandom distribution of residuals and a negative (physically meaningless) value of *B*, indicating that the model greatly underestimated the degree of association. Fitting the DTHO model to 0.4−1.5 M NaCl data gave similar results, with *B* values several orders of magnitude smaller than the value obtained at 0.1 M NaCl. The data were then fitted with the SEK models, which describe various

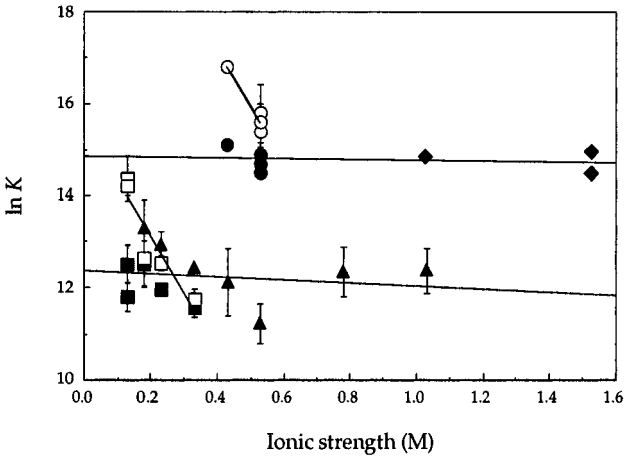

FIGURE 6: Comparison of the association behavior of erythroid and brain spectrin in 0.4−1.5 M NaCl. The data points represent the values of the equilibrium constants estimated from nonlinear regression fitting of the SEK models to Ω versus concentration plots obtained for brain spectrin at 20 °C: K_{24} (○) and K_{iso} (●) of the SEK 3 model and K (▲) of the SEK 1 and SEK 4 models (see Experimental Procedures for details). The equilibrium constants for erythroid spectrin, obtained by Cole and Ralston (1992) at 30 °C, are also shown: K_{24} (□) and K_{iso} (■) of the SEK 3 model and K (▲) of the SEK 4 model. The solid lines represent unweighted linear regression fits for (i) K_{24} from the SEK 3 model and (ii) K_{iso} from the SEK 3 model and K from the SEK 1 and SEK 4 models. For brain spectrin, the error bars represent the standard errors of the equilibrium constants obtained from nonlinear regression analysis of Ω function data combined from three loading concentrations of protein. For the erythroid spectrin data, the error bar for each point represents the standard error of the mean value of the equilibrium constant obtained from fitting the data from the three loading concentrations separately (*33*).

types of indefinite self-association (*31*; see Experimental Procedures). For brain spectrin in 0.4−1.0 M NaCl at 20 °C, a protomer molar mass (M_1) of 559 000 g/mol (equivalent to the dimer) was used and both the SEK I and SEK 3 models were tested. At concentrations of 1.5 M NaCl, the SEK 4 model was also tested, in order to take into account possible dissociation to monomer. For this model, a value for M_1 of 280 000 g/mol was used.

For brain spectrin in NaCl at concentrations of 0.4−0.5 M, the SEK 3 model, which defines a separate K_{24} and K_{iso}, gave the best fit to the data (Figure 6). At higher NaCl concentrations, however, K_{24} decreased until it became equal to K_{iso}, and the SEK 1 model, which describes all steps by a single K, was more appropriate (Figure 6). At 1.5 M NaCl, dissociation of dimers to monomers occurred at protein concentrations of less than 0.1 g/L. In this case, the Ω data were fitted best by the SEK 4 model, which returned a K_{12} of 7×10^6 M^{-1} for the formation of the dimer and a K for the sequential addition of heterodimers which was similar to that obtained at 1.0 M NaCl.

Figure 6 also compares the equilibrium constants of brain and erythroid spectrin over a range of ionic strengths [spectrin data obtained from Cole and Ralston (*33*)]. At ≥0.4 M NaCl, the equilibrium constants for brain spectrin are ∼15-fold higher than those for erythroid spectrin. The convergence of K_{24} and K_{iso} which occurs at ≥0.5 M NaCl for brain spectrin occurs with erythroid spectrin at only ∼0.2 M. Similarly, the dissociation of brain spectrin dimers to monomers, which is detectable at 1.5 M NaCl for brain spectrin, occurs in erythroid spectrin at only 0.3 M NaCl.

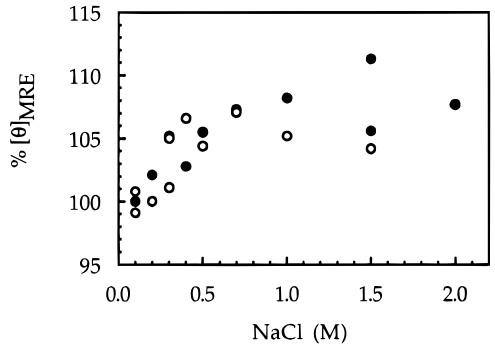

FIGURE 7: Percentage change in mean residue ellipticity, $[\theta]_{MRE}$, at 222 nm measured from the CD spectra of erythroid spectrin (○) and brain spectrin (●) in 0.2−2.0 M NaCl, relative to the $[\theta]_{MRE}$ at 0.1 M NaCl.

The marked difference in the values of the equilibrium constants describing the self-association of brain and erythroid spectrin is not due to the differing temperatures at which the data were collected (20 and 30 °C, respectively). Although most of the brain spectrin data were obtained at 20 °C, experiments at 30 °C produced equilibrium constants that were comparable to those obtained at 20 °C and were still at least 1 order of magnitude larger than those of erythroid spectrin at the same ionic strength. Similarly, experiments on erythroid spectrin at 20 °C produced results consistent with those at 30 °C.

Circular Dichroism Analysis of Spectrin at High Ionic Strengths. The dependence of the α-helical content of erythroid and brain spectrin on ionic strength was measured by changes in the mean residue ellipticity at 222 nm. As Figure 7 shows, the magnitude of the ellipticity at 222 nm increased by 5−10% with an increase in NaCl from 0.1 to 1.5 M at 25 °C. The data therefore indicate a small increase in the percentage of α-helix with increasing salt for both erythroid and brain spectrin.

DISCUSSION

In a comparison of erythroid and brain spectrin association using electron microscopy and nondenaturing PAGE, it was found that, while erythroid spectrin formed oligomers ranging from dimers to octamers, brain spectrin appeared only as a tetramer (*20*). Our analysis of brain spectrin in 0.1 M NaCl using sedimentation equilibrium shows that it is exclusively tetrameric *at equilibrium* over a wide range of temperatures (18−37 °C, Figure 1). At 30 °C, brain spectrin remains tetrameric at ionic strengths between 0.1 and 0.3 M. However, at ionic strengths of ≥0.4 M, brain spectrin tetramers are destabilized, and the protein is able to form both dimers and higher oligomers in a manner qualitatively similar to that seen with erythroid spectrin (Figure 5). In fact, the association of both spectrins can be described by the SEK models of indefinite self-association (Figure 6).

The association behavior of both spectrins may be interpreted using the ring closure model of Morris and Ralston (*10*) (Figure 8). Electron microscopy studies indicate that the erythroid spectrin heterodimer is mostly in the closed form, whereby the binding sites of the α and β subunits form an intradimer bond (*42*). Self-association of dimers requires the open form of the dimer, however, and the equilibrium between the open and closed form of the dimer is described by a ring closure constant, K_{r2}. The interaction of two open

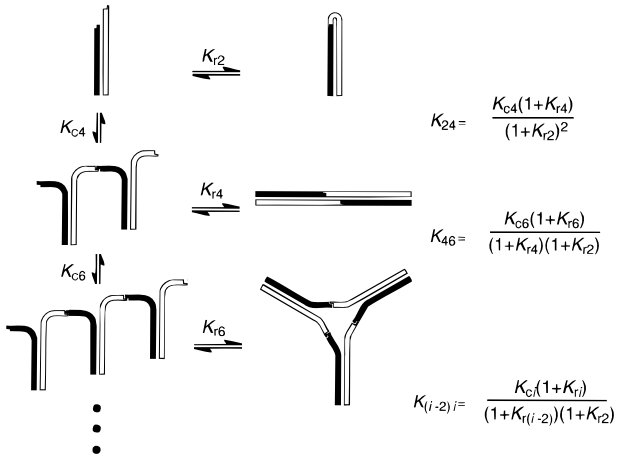

FIGURE 8: Ring closure model for the self-association of spectrin (*10*). The K_{ci}'s represent the association constants for the addition of an open dimer to an open ($i - 2$)-mer which forms an open i-mer ($i = 4, 6, 8, 10$, etc.). The K_{r2} and K_{ri} represent the equilibrium constants for the formation of the ring, or closed, form of an oligomer from the open, or chain, form. The $K_{(i-2)i}$ are the measured equilibrium constants for the formation of an i-mer from an ($i - 2$)-mer and a dimer summed over both the open and closed forms of the participating species.

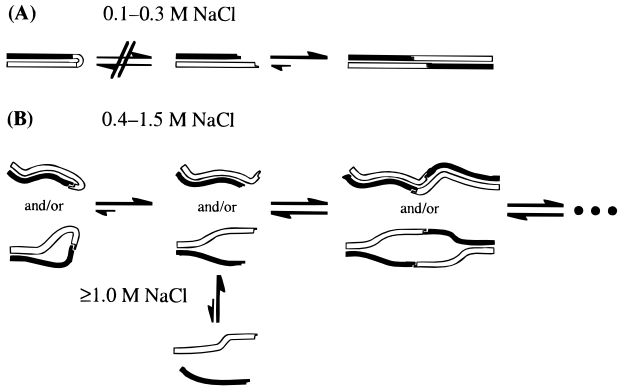

FIGURE 9: Model of the salt-dependent changes in brain spectrin self-association. (A) At 0.1−0.3 M NaCl, the rigidity of the brain spectrin subunits in the dimer allows self-association to proceed only as far as the tetramer and prevents the dimer from closing and forming a ring structure. In principle, dimer−tetramer exchange can occur. However, the tetramer is highly thermodynamically favored with respect to the open dimer and is the only species detectable over the range of concentrations accessible in our experiments. (B) In 0.4−1.5 M NaCl, the heads of the α and β subunits can move somewhat independently of one another. This may be the result of greater subunit flexibility (upper diagrams) and/or weakening of the side-to-side associations resulting in "unzipping" of the chains (lower diagrams). The increased independent movement of the subunit heads allows the formation of oligomers larger than the tetramer and also allows limited formation of closed, kinetically trapped dimers. At ≥1.0 M NaCl, the side-to-side interactions are weakened to the point where dissociation of dimers to monomers is detectable.

dimers which forms an open tetramer is described by a chain constant, K_{c4}, and indefinite association proceeds by the sequential addition of open dimers to open oligomers, each step described by a chain constant, K_{ci}, ($i = 4, 6, 8, 10$, etc.). Each of the erythroid spectrin open oligomers is flexible enough to close to the ring form such that all of the binding sites are satisfied, and these closures are described by ring closure constants, K_{ri}. Such closed oligomers have been observed in the electron microscope (*14*).

The ring closure model has been used to interpret the mechanism of erythroid spectrin self-association (*10, 39*). For example, in conditions where the SEK 3 model describes the self-association, the observed equilibrium constant for the formation of the tetramer, K_{24}, is larger than the constants, K_{iso}, describing the formation of all larger oligomers. This can be attributed to the greater conformational strain associated with closing the dimer, that is, the difficulty of bending the longer α subunit back upon itself in order to bind to the β subunit (*7, 39*). This conformational strain reduces the ring closure constant for the dimer, K_{r2}, with respect to the other ring closure constants, which in turn increases the value of K_{24} with respect to the other constants, K_{iso} (*10*, Figure 8).

Thus, the mode of erythroid spectrin self-association is heavily dependent on the intrinsic flexibility and the independent movement of its α and β subunits; electron micrographs of erythroid spectrin oligomers (*14, 43*) demonstrate that partial separation of the subunits occurs when the heads of the subunits in one dimer bend outward to form contacts with two other dimers. It can therefore be predicted that a stiffer, more rod-like form of spectrin will have the following properties (Figure 9A). (i) The dimers will have difficulty in closing to a ring structure, and the open form of the dimer will predominate. (ii) If the dimers can self-associate, then the largest species that will form will be the tetramer, the stiff chains with their coupled motion preventing the self-association interface from opening up and accommodating further dimers. (iii) If the association between two dimers is sufficiently strong, then effectively, the only species detectable in solution will be the tetramer. (iv) As the dimer is mostly in the open form, there will be no kinetic restrictions to dimer−tetramer association.

These predictions are consistent with the behavior of brain spectrin we have observed using sedimentation equilibrium and sedimentation velocity techniques. Brain spectrin's very large frictional ratio and its morphology as observed in EM studies (*20*) both indicate that it is a stiffer, more rod-like molecule than erythroid spectrin. Brain spectrin is exclusively tetrameric at sedimentation equilibrium in 0.1 M NaCl over the temperature range of 18−37 °C (Figure 1). Under conditions where the tetramer can dissociate (≥0.3 M NaCl), brain spectrin forms a boundary in sedimentation velocity experiments whose $s_{20,w}$ value lies between those of the tetramer and dimer (Figure 2). This boundary represents a rapid dimer−tetramer exchange that is not kinetically restricted, even at 2 °C. The dimers involved in this rapid exchange are likely to be in the open state. This is supported by other experiments which show that brain spectrin, like erythroid spectrin, can also form a separate boundary containing kinetically trapped dimers during sedimentation at 20 °C (Figure 4). The dimer in this boundary is likely to be in the closed form.

At salt concentrations of ≥0.4 M, brain spectrin is able to associate in a manner qualitatively similar to that of erythroid spectrin, and the self-association of both types of spectrin can be modeled using the ring closure model of Morris and Ralston (*10*) (Figure 8). The ability of brain spectrin to form a wide range of oligomers in ≥0.4 M NaCl indicates that the self-association sites at the head of the α and β subunits can now move independently of one another (Figure 9B). At 0.4−0.5 M NaCl, the brain spectrin tetramer is still favored relative to other oligomers, as shown by the fact that K_{24} is higher than K_{iso} (Figure 6). However, K_{24}

decreases with ionic strength until it becomes equal to K_{iso}, indicating a relative destabilization of the brain spectrin tetramer due to the increasingly independent movement of the chains. Ultimately, increasing salt results in the detectable dissociation of dimers to monomers starting at ~1.5 M NaCl. Note that for erythroid spectrin similar changes are observed but different concentrations of salt are required (Figure 6). Erythroid spectrin is flexible enough to form a range of oligomers even in 0.1 M NaCl, and only 0.2 M NaCl is required to destabilize the tetramer to the point where $K_{24} = K_{iso}$. The dissociation of dimers to monomers occurs in as little as 0.3 M NaCl.

Thus, the salt-dependent changes in the association behavior of erythroid and brain spectrin are qualitatively similar but quantitatively different. In particular, at all ionic strengths tested, the equilibrium constants K_{24}, K_{iso}, and K describing brain spectrin association are around 15-fold higher than those describing erythroid spectrin association (Figure 6). This result supports our sedimentation velocity data which indicate that brain spectrin more readily forms open dimers than erythroid spectrin; since all of the association steps require the addition of open dimers, a tendency for brain spectrin dimers to be in the open form will greatly favor higher association. The ring closure model equations (Figure 8) can be used to demonstrate this; when the open form of the dimer is thermodynamically favored, the value of K_{r2} will decrease and the values of K_{24}, K_{iso}, and K will increase. (It is possible that brain spectrin has a larger unitary free energy for chain formation, which would result in larger values of K_{ci} compared to those for erythroid spectrin. However, this would not change the values of the measured equilibrium constants since the ring closure constants, K_{r2} and K_{ri}, also describe the head-to-head association of an α and a β subunit. Thus, the effect of an increase in the K_{ci} on the measured K would be canceled by a proportional increase in K_{r2} and K_{ri}.)

Implications for Interactions Stabilizing Erythroid and Brain Spectrin. There are likely to be two factors determining the stability and flexibility of spectrin oligomers: (a) the number and strength of the side-to-side interactions between the α and β subunits and (b) the flexibility of the individual monomer chains. Interpretation of our sedimentation equilibrium and velocity data in terms of the ring closure model can provide information on the nature and location of interactions stabilizing the quaternary structure of erythroid and nonerythroid spectrins.

As discussed above, the values of the equilibrium constants describing the self-association of brain spectrin are consistently higher than those for erythroid spectrin and indicate a smaller tendency of brain spectrin to form closed dimers. Under conditions where a single value of K can be used to describe the sequential addition of heterodimers, the value of this K is ~15-fold higher for brain spectrin. This remains unchanged even when the side-to-side interactions are weak enough to allow dissociation of dimers to monomers. In particular, when both erythroid and brain spectrin have the same equilibrium constant for the formation of dimer from the α and β subunits ($K_{12} = 7 \times 10^6$ M^{-1}), the value of K describing the sequential addition of dimers remains ~15-fold higher for brain spectrin. Together, the data indicate that the smaller tendency of brain spectrin to form closed dimers relative to that of erythroid spectrin is not due to stronger side-to-side association in brain spectrin, but to a smaller *intrinsic flexibility* of the α and/or β subunits of brain spectrin. Furthermore, the ~15-fold difference between erythroid and brain spectrin K's is independent of salt, and therefore, the forces controlling the intrinsic flexibility of spectrin subunits are not electrostatic. They may, instead, be hydrophobic. Hydrophobic interactions have been postulated by Yan *et al.* (*3*) to occur between consecutive *Drosophila* spectrin repeat units and have also been postulated to influence the flexibility of the α and β subunits of spectrin (*44*).

The eventual dissociation of both erythroid and brain spectrin to monomers indicates that the side-to-side association of the α and β subunits is weakened with increasing ionic strengths. This may arise as an indirect effect due to the loss of secondary structure. However, the CD data show that there is no net loss of spectrin α-helix with increasing ionic strengths (Figure 7). Alternatively, the side-to-side association may be weakened by an increase in flexibility of the monomer chains, but again, the erythroid spectrin data indicate that the disruption of side-to-side association cannot be due solely to this. For example, at a moderate ionic strength (0.5 M) at 20 °C, where the conformational strain of dimer closure is still large enough to result in kinetic restrictions on dimer−tetramer exchange (Figure 3A), the side-to-side association is weakened, allowing measurable dissociation of dimers to monomers at equilibrium. In contrast, in conditions where erythroid spectrin is highly flexible and there are greatly reduced kinetic restrictions to closed dimer formation (e.g., at 37 °C in 0.16 M salt; *39*), there is no detectable dissociation of dimers (*11*). Taken together, the data suggest that the ionic strength-dependent dissociation of dimers to monomers is due primarily to disruption of electrostatic side-to-side interactions between the α and β subunits, rather than to increased subunit flexibility.

REFERENCES

1. Repasky, E. A., Granger, B. L., and Lazarides, E. (1982) *Cell 29,* 821−833.
2. Speicher, D. W., and Marchesi, V. T. (1984) *Nature 311,* 177−180.
3. Yan, Y., Winograd, E., Viel, A., Cronin, T., Harrison, S. C., and Branton, D. (1993) *Science 262,* 2027−2030.
4. Pascual, J., Pfuhl, M., Rivas, G., Pastore, A., and Saraste, M. (1996) *FEBS Lett. 383,* 201−207.
5. Speicher, D. W., Weglarz, L., and DeSilva, T. M. (1992) *J. Biol. Chem. 267,* 14775−14782.
6. Viel, A., and Branton, D. (1994) *Proc. Natl. Acad. Sci. U.S.A. 91,* 10839−10843.
7. Speicher, D. W., DeSilva, T. M., Speicher, K. D., Ursitti, J. A., Hembach, P., and Weglarz, L. (1993) *J. Biol. Chem. 268,* 4227−4235.
8. Kennedy, S. P., Weed, S. A., Forget, B. G., and Morrow, J. S. (1994) *J. Biol. Chem. 269,* 11400−11408.
9. Ungewickell, E., and Gratzer, W. (1978) *Eur. J. Biochem. 88,* 379−385.
10. Morris, M., and Ralston, G. B. (1989) *Biochemistry 28,* 8561−8567.
11. Henniker, A., and Ralston, G. B. (1994) *Biophys. Chem. 52,* 251−258.
12. Morrow, J. S., and Marchesi, V. T. (1981) *J. Cell. Biol. 88,* 463−468.
13. Morrow, J. S., Haigh, W. B., and Marchesi, V. T. (1981) *J. Supramol. Struct. 17,* 275−287.
14. Liu, S.-C., Windisch, P., Kim, S., and Palek, J. (1984) *Cell 37,* 587−594.

15. Morris, M., and Ralston, G. B. (1984) *Biochim. Biophys. Acta 788*, 132−137.
16. Glenney, J. R., Jr., Glenney, P., Osborn, M., and Weber, K. (1982) *Cell 28*, 843−854.
17. Bennett, V., Davis, J., and Fowler, V. E. (1982) *Nature 299*, 126−131.
18. Davis, J., and Bennett, V. (1983) *J. Biol. Chem. 258*, 7757−7766.
19. Goodman, S. R., Zagon. I. S., Whitfield, C. F., Casoria, L. A., McLaughlin, P. J., and Laskiewicz, T. L. (1983) *Cell Motil. 3*, 635−647.
20. Harris, A. S., Green, L. A. D., Ainger, K. J., and Morrow, J. S. (1985) *Biochim. Biophys. Acta 830*, 147−158.
21. Morris, S. A., Eber, S. W., and Gratzer, W. B. (1989) *FEBS Lett. 244*, 68−70.
22. Bennett, V., Baines, A. J., and Davis, J. (1986) *Methods Enzymol. 134*, 55−69.
23. Ralston, G. B., Teller, D. C., and Bukowski, T. (1989) *Anal. Biochem. 178*, 198−201.
24. Teller, D. C. (1973) *Methods Enzymol. 27*, 346−441.
25. Babul, J., and Stellwagen, E. (1969) *Anal. Biochem. 28*, 216−221.
26. Milthorpe, B. K., Jeffrey, P. D., and Nichol, L. W. (1975) *Biophys. Chem. 3*, 169−176.
27. Ma, Y., Zimmer, W. E., Reiderer, B. M., and Goodman, S. R. (1993) *Mol. Brain Res. 18*, 87−99.
28. Wasenius, V.-M., Saraste, M., Salven, P., Eramaa, M., Holm, L., and Lehto, V.-P. (1989) *J. Cell. Biol. 108*, 79−93.
29. Laue, T. M., Shah, B. D., Ridgeway, T. M., and Pelletier, S. L. (1992) in *Analytical Ultracentrifugation in Biochemistry and Polymer Science* (Harding, S. E., Rowe, A. J., and Horton, J. C., Eds.) pp 90−125, The Royal Society of Chemistry, Cambridge.
30. Ralston, G. B., and Morris, M. B. (1992) in *Analytical Ultracentrifugation in Biochemistry and Polymer Science* (Harding, S. E., Rowe, A. J., and Horton, J. C., Eds.) pp 253−274, The Royal Society of Chemistry, Cambridge.
31. Adams, E. T., Jr., Tang, L.-H., Sarquis, J. L., Barlow, G. H., and Norman, W. M. (1978) in *Physical Aspects of Protein Interactions* (Catsimpoolas, N., Ed.) pp 1−55, Elsevier/North Holland, Amsterdam.
32. Morris, M. B., and Ralston, G. B. (1985) *Biophys. Chem. 23*, 49−61.
33. Cole, N., and Ralston, G. B. (1992) *Biochim. Biophys. Acta 1121*, 22−30.
34. Adams, E. T., Jr., and Fujita, H. (1963) in *Ultracentrifugal Analysis in Theory and Experiment* (Williams, J. W., Ed.) pp 119−129, Academic Press, New York.
35. Cleland, W. W. (1967) *Adv. Enzymol. Relat. Areas Mol. Biol. 21*, 1−32.
36. Johnson, M. L., Correia, J. A., Yphantis, D. A., and Halvorson, H. R. (1981) *Biophys. J. 36*, 575−588.
37. Schmid, F. X. (1990) in *Protein Structure: A Practical Approach* (Creighton, T. E., Ed.) pp 280−285, IRL Press, Oxford.
38. Tanford, C. (1961) *Physical Chemistry of Macromolecules*, Wiley, New York.
39. DeSilva, T. M., Peng, K.-C., Speicher, K. D., and Speicher, D. W. (1992) *Biochemistry 31*, 10872−10878.
40. Stafford, W. F. (1992) in *Analytical Ultracentrifugation in Biochemistry and Polymer Science* (Harding, S. E., Rowe, A. J., and Horton, J. C., Eds.) pp 359−393, The Royal Society of Chemistry, Cambridge.
41. Stafford, W. F. (1994) *Methods Enzymol. 240*, 478−501.
42. Shotton, D. M., Burke, B. E., and Branton, D. (1979) *J. Mol. Biol. 131*, 303−329.
43. Liu, S.-C., Derick, L. H., and Palek, J. (1987) *J. Cell Biol. 104*, 527−536.
44. Vertessy, B. G., and Steck, T. L. (1989) *Biophys. J. 55*, 255−262.

BI970186N